



# Uncertainty in water transit time estimation with StorAge Selection functions and tracer data interpolation

Arianna Borriero<sup>1</sup>, Rohini Kumar<sup>2</sup>, Tam V. Nguyen<sup>1</sup>, Jan H. Fleckenstein<sup>1,3</sup>, and Stefanie R. Lutz<sup>4</sup>

<sup>1</sup>Department of Hydrogeology, Helmholtz-Centre for Environmental Research - UFZ, Leipzig, Germany

<sup>2</sup>Department of Computational Hydrosystems, Helmholtz-Centre for Environmental Research - UFZ, Leipzig, Germany

<sup>3</sup>Bayreuth Centre of Ecology and Environmental Research, University of Bayreuth, Bayreuth, Germany

<sup>4</sup>Copernicus Institute of Sustainable Development, Department of Environmental Sciences, Utrecht University, Utrecht, the Netherlands

**Correspondence:** Arianna Borriero (arianna.borriero@ufz.de)

**Abstract.** Transit time distributions (TTDs) of streamflow are useful descriptors for understanding flow and solute transport in catchments. Catchment-scale TTDs can be modeled using tracer data (e.g.,  $\delta^{18}\text{O}$ ; oxygen isotopes) in inflow and outflows, with StorAge Selection (SAS) functions. However, tracer data are often sparse in space and time, so they can be interpolated to increase their spatio-temporal resolution. Also, SAS functions can be parameterized with different forms, but there is no general agreement on which one should be used. Both of these aspects induce uncertainty in the simulated TTDs, and the individual uncertainty sources as well as their combined effect have not been fully investigated. This study provides a comprehensive analysis of the TTD uncertainty resulting from twelve model setups obtained by combining different interpolation schemes for  $\delta^{18}\text{O}$  in precipitation, and distinct SAS functions. Furthermore, we evaluated the value of the young water fraction ( $F_{yw}$ ) as an additional constraint for the TTD uncertainty. For each model setup, we found behavioral solutions with satisfactory model performances for instream  $\delta^{18}\text{O}$  (Kling-Gupta Efficiency,  $\text{KGE} > 0.57$ ). Differences in KGE values were statistically significant, thus showing the relevance of the chosen setup for simulating TTDs. We found a large uncertainty in the simulated TTDs, with a 90% confidence interval varying between 286 and 895 days across all tested setups. Uncertainty in TTDs was mainly associated with the temporal interpolation of  $\delta^{18}\text{O}$  in precipitation, time-variant SAS function and low flow conditions. The use of  $F_{yw}$  as an additional constraint substantially reduced the uncertainty in the predicted TTDs by up to 49%. We discussed the implications of these results with respect to the study area and the SAS framework, in order to identify ways to improve uncertainty characterization and water age simulations in TTD-based models.

## 1 Introduction

Understanding how catchments store and release water of different ages has significant implications for flow and solute transport as water ages encapsulate information about flowpaths characteristics (McGuire and McDonnell, 2006; Botter et al., 2011), contact time of solutes with the soil matrix (Benettin et al., 2015a; Hrachowitz et al., 2016), and vulnerability assessment (Kumar et al., 2020). This plays an important role for water resources protection and management, as well as requires a tool that can effectively describe catchment-scale transport processes (Rinaldo and Marani, 1987). The water age in outflows is commonly



referred to as transit time (TT), i.e., the time elapsed between the entry of a water parcel into the catchment via precipitation and its exit via streamflow or evapotranspiration. Accordingly, the transit time distribution (TTD) describes the whole spectrum of the transit times in outflows (Botter et al., 2005; Van der Velde et al., 2010). Early studies have often assumed simplified steady-state transport models, resulting in time-invariant TTDs (Niemi, 1977; Rinaldo et al., 2006). However, experimental simulations showed that TTDs are time-variant due to variability in meteorological forcing (Botter et al., 2010; Hrachowitz et al., 2010; Heidbüchel et al., 2020). A promising tool for representing time-variant TTDs are StorAge Selection (SAS) functions, which describe how catchments selectively remove water of different ages from storage to outflows (Rinaldo et al., 2015; Harman, 2019). SAS functions have led to a new framework of non-stationary transport models based on water age, which have been successfully applied in various transport modelling studies (Benettin et al., 2015b; Quéloz et al., 2015; Kim et al., 2016; Lutz et al., 2017; Wilusz et al., 2017; Nguyen et al., 2021).

Model-based TTDs are subjected to uncertainty which limits their ability for decision support. In general, model prediction uncertainty stems from model inputs, structure, and parameters (Beven and Freer, 2001). As TTDs are not directly observable, conservative environmental tracers (e.g.,  $\delta^{18}\text{O}$ ; oxygen isotopes) in inflow and outflows are commonly used to infer water ages (Hrachowitz et al., 2013; Birkel and Soulsby, 2015; Stockinger et al., 2015). Long-term, high-frequency tracer data with an appropriate spatial distribution are generally recommended for sufficient understanding of the TTDs dynamics across a wide range of fast and heterogeneous hydrological behaviors (Kirchner et al., 2004; Danesh-Yazdi et al., 2016; von Freyberg et al., 2017). Therefore, the lack of an appropriate tracer data coverage can prevent our understanding of the TTDs dynamics at the desired resolution (McGuire and McDonnell, 2006). Further uncertainty emerges from the model structure due to the difficulty in representing physical processes because of our incomplete knowledge of complex reality (Ajami et al., 2007). Finally, specification of model parameters is also an important source of uncertainty (Beven, 2006; Kirchner, 2006), as the best-fit parameters may suffer from equifinality (Schoups et al., 2008).

A few studies have investigated the uncertainty in the estimated TTDs with SAS models. Danesh-Yazdi et al. (2018) and Jing et al. (2019) have analysed the effect of the interactions between distinct flow domains, external forcing and recharge rate on TTDs. Several works (Benettin et al., 2017; Wilusz et al., 2017; Rodriguez et al., 2018, 2021) have explored model parameter uncertainty, and suggested that additional types of tracers, data on physical characteristics of the catchment, and parsimonious parameterization may help to further reduce parameters uncertainty. More recently, Buzacott et al. (2020) investigated how gap-filling of the  $\delta^{18}\text{O}$  record in precipitation propagated uncertainty into the simulated mean water transit time (MTT), i.e., the average time it takes for water to leave the catchment (McDonnell et al., 2010).

Despite the studies cited above, there are other aspects causing uncertainty in the simulated TTDs, which have not yet been fully addressed. First, isotope data are generally sparse globally in space and time (von Freyberg et al., 2022), due to laborious and costly sampling campaigns limited to well-equipped areas (Tetzlaff et al., 2018). For this reason, spatio-temporal interpolation of the isotope composition in precipitation can be used to get greater data coverage, required for modelling purposes. Second, SAS functions, employed to model TTDs, must be parameterized, and commonly used parameterizations are the power law (Benettin et al., 2017; Asadollahi et al., 2020) and beta distribution (van der Velde et al., 2012; Drever and Hrachowitz, 2017). However, there is no general agreement on which SAS function should be used as the hydrological



processes which control subsurface mixing, hence TTDs dynamics, are distinct across different catchments. Therefore, the most convenient approach is to simply rely on one parameterization over another, and estimate its parameters (Harman, 2015).  
60 Both of these aspects induce model input, structure and parameter uncertainty in the simulated TTDs. To date, the individual uncertainty sources and their combined effect on the modeled TTDs have not been adequately discussed.

To reduce the estimated TTD uncertainty, various studies have suggested combining stable and decaying tracers (Duvert et al., 2016), the latter best imparting old water ages. Others have proposed high sampling resolution (e.g., daily) to provide better insights into short-term events (Timbe et al., 2015). Nonetheless, when long-term, high frequency tracer data are scarce,  
65 methods that rely on short-term, low frequency data can become an alternative option to reduce TTD uncertainty. One such example is the young water fraction ( $F_{yw}$ ; streamflow ratio younger than 2-3 months (Kirchner, 2016a)), which can be easily retrieved from low frequency tracer data covering relatively short period. The estimation of  $F_{yw}$  is based on the amplitude ratio of the seasonal cycles in stable water isotopes in precipitation and streamflow.  $F_{yw}$  represents an alternative descriptor for TTD, a robust metric under both spatially heterogeneous and non-stationary conditions, as well as less prone to a large aggregation  
70 bias than MTTs (Kirchner, 2016b). Benettin et al. (2017) proposed to use  $F_{yw}$  to restrict model parameter values, while Lutz et al. (2018) implemented it as an additional constraint in the calibration of gamma-distributed TTDs. However, to the best of our knowledge, no studies have attempted to employ  $F_{yw}$  for constraining predictive uncertainties in SAS-based TTDs.

This study bridges the aforementioned gaps by specifically exploring the combined effect of sparse input tracer data and model parameterizations on the simulated TTDs. We investigated TTD uncertainty using a SAS-based catchment-scale trans-  
75 port model applied to the Upper Selke catchment, Germany. We evaluated TTDs resulting from twelve model setups obtained by combining distinct interpolation techniques of  $\delta^{18}\text{O}$  in precipitation, and parameterizations of SAS functions. For each model setup, we searched for behavioral parameter sets (i.e., those providing acceptable predictions) based on model performance for instream  $\delta^{18}\text{O}$ . Afterwards, we evaluated the sources of uncertainty, as well as their combined effects, in the resulting TTDs and, finally, we tested whether and to what extent  $F_{yw}$  could provide valuable information to further constrain the un-  
80 certainty. Overall, our results provide new insights into the uncertainty characterization of TTDs, particularly in the absence of high-frequency tracer data, and the use of SAS functions.

## 2 Study area and data

The Upper Selke catchment is located in the Harz Mountains in Saxony-Anhalt, central Germany (Fig. 1). The study site is part of the Bode region, an intensively monitored area within the TERENO (TERrestrial ENvironmental Observatories;  
85 Wollschläger et al., 2017) network. The catchment has a drainage area of 184 km<sup>2</sup>, the altitude ranges between 184 and 594 m above mean sea level, and the mean slope is 7.65%. Land use is dominated by forest (broadleaf, coniferous and mixed forest) and agricultural land (winter cereals, rapeseed and maize), representing 72% and 21% of the catchment, respectively. The soil is largely composed of cambisols and the underlying geology consists of schist and claystone, resulting in a predominance of relatively shallow flowpaths (Dupas et al., 2017; Yang, J. et al., 2018).



90 Daily hydroclimatic and monthly tracer data in the Upper Selke were available for the period between February 2013 and  
May 2015. Precipitation (P) was taken from the German weather service, while discharge (Q) and evapotranspiration (ET) were  
simulated data obtained from the mesoscale Hydrological Model (mHM; (Samaniego et al., 2010; Kumar et al., 2013)) since  
continuous measurements were not available for the given outlet and period. A thorough evaluation of mHM performance for  
past measurements have been conducted in previous studies (Zink et al., 2017; Yang, X. et al., 2018; Nguyen et al., 2021). The  
95 average annual P, Q and ET are 703, 108, 596 mm, respectively. The area is characterized by high flow during November-May  
(average Q = 0.88 m<sup>3</sup>/s) and low flow during June-October (average Q = 0.42 m<sup>3</sup>/s). Evapotranspiration is higher in June (109  
mm/month) and lower in December (10 mm/month). The average monthly temperature ranges from -0.7°C in January to 17°C  
in July. The  $\delta^{18}\text{O}$  values in precipitation ( $\delta^{18}\text{O}_P$ ) and in streamflow ( $\delta^{18}\text{O}_Q$ ) at monthly resolution were taken from Lutz et al.  
(2018) (Fig. S1).  $\delta^{18}\text{O}_P$  were used in the form of "raw" (i.e., values collected at the catchment outlet) and processed (i.e.,  
100 spatially interpolated using kriging) data (Section 3.2). The variability in  $\delta^{18}\text{O}_P$  was larger than  $\delta^{18}\text{O}_Q$  because of the damped  
precipitation signal due to mixing and dispersion within the catchment. Temperature dependence caused more depleted (i.e.,  
more negative)  $\delta^{18}\text{O}_P$  in winter than in summer (Fig. S1).

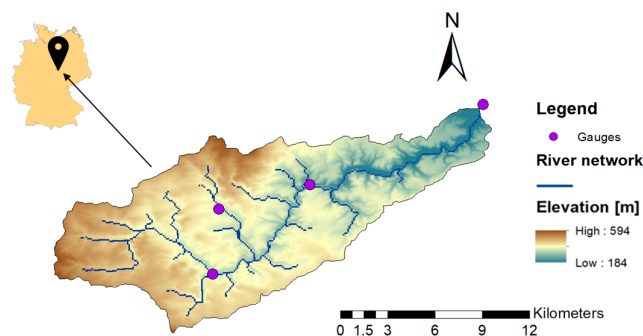


**Figure 1.** Upper Selke catchment with precipitation sampling points (purple dots), river network (blue lines), and elevation in meters above sea level as colored map; location of the Upper Selke catchment in Germany (upper left corner).

### 3 Methods

#### 3.1 Catchment-scale transport model

105 In this study, we used the *tran-SAS* model (Benettin and Bertuzzo, 2018) for describing the catchment-scale water mixing and  
solute transport based on SAS functions. The catchment was conceptualized as a single storage  $S(t)$  (mm), whose water-age  
balance can be expressed as follows (Benettin and Bertuzzo, 2018):

$$S(t) = S_0 + V(t) \quad (1)$$



$$110 \quad \frac{\partial S_T(T, t)}{\partial t} + \frac{\partial S_T(T, t)}{\partial T} = P(t) - Q(t) \cdot \Omega_Q(S_T, t) - ET(t) \cdot \Omega_{ET}(S_T, t) \quad (2)$$

$$\text{Initial condition: } S_T(T, t = 0) = S_{T_0} \quad (3)$$

$$\text{Boundary condition: } S_T(0, t) = 0 \quad (4)$$

where  $S_0$  (mm) is the initial storage,  $V(t)$  (mm) are the storage variations,  $P(t)$  (mm/d),  $Q(t)$  (mm/d), and  $ET(t)$  (mm/d) are precipitation, discharge and evapotranspiration, respectively,  $S_T(T, t)$  (mm) is the age-ranked storage,  $S_{T_0}$  (mm) is the initial age-ranked storage, and  $\Omega_Q(S_T, t)$  (-) and  $\Omega_{ET}(S_T, t)$  (-) are the cumulative SAS functions for  $Q$  and  $ET$ , respectively.

By definition, the TTD of streamflow  $p_Q(T, t)$  ( $d^{-1}$ ) is calculated as follows (Benettin and Bertuzzo, 2018):

$$p_Q(T, t) = \frac{\partial \Omega_Q(S_T, t)}{\partial S_T} \cdot \frac{\partial S_T}{\partial T} \quad (5)$$

The isotopic signature in streamflow  $C_Q(t)$  (‰) can be obtained from (Benettin and Bertuzzo, 2018):

$$C_Q(t) = \int_0^{+\infty} C_S(T, t) \cdot p_Q(T, t) \cdot dT \quad (6)$$

120 where  $C_S(T, t)$  (‰) is the isotopic signature of a water parcel in storage. Equations 5 and 6 also apply for  $ET$ .

In this study, we tested three SAS parameterizations: the power law time-invariant (PLTI; Eq. 7 (Queloz et al., 2015)), power law time-variant (PLTV; Eq. 8 (Benettin et al., 2017)), and beta distribution (BETA; Eq. 9 (Drever and Hrachowitz, 2017)). They can be expressed as probability density functions in terms of the normalized age-ranked storage  $P_S(T, t)$  (-):

$$\omega(P_S(T, t), t) = k \cdot (P_S(T, t))^{k-1} \quad (7)$$

$$125 \quad \omega(P_S(T, t), t) = k(t) \cdot (P_S(T, t))^{k(t)-1} \quad (8)$$

$$\omega(P_S(T, t), t) = \frac{(P_S(T, t))^{\alpha-1} \cdot (1 - P_S(T, t))^{\beta-1}}{B(\alpha, \beta)} \quad (9)$$

The parameters  $k$ ,  $\alpha$  and  $\beta$  determine the catchment's water age preference for outflow, while  $B(\alpha, \beta)$  is the two-parameter beta function. If  $k < 1$ , or if  $\alpha < 1$  and  $\beta > 1$ , the system tends to discharge young water. If  $k > 1$ , or if  $\alpha > 1$  and  $\beta < 1$ , the catchment preferably releases old water. The case of  $k = 1$  or  $\alpha = \beta = 1$  describes no selection preference (i.e., complete water mixing). PLTV is characterized by  $k(t)$  varying linearly over time between two extremes  $k_1$  and  $k_2$  as a function of the catchment wetness  $wi$  (-), i.e.,  $wi(t) = (S(t) - S_{min}) / (S_{max} - S_{min})$ , where  $S_{min}$  and  $S_{max}$  are the minimum and maximum storage values over the entire period.

### 3.2 Interpolation techniques for $\delta^{18}O$ in precipitation

We tested the model with two spatial and two temporal interpolation methods of tracer data to explore the TTD uncertainty resulting from model input. To evaluate the effect of the spatial interpolation, we first set a base case using monthly raw  $\delta^{18}O_p$  taken from Lutz et al. (2018), corresponding to the values collected at the catchment outlet (i.e., Meisdorf station).



Second, we used the spatially interpolated  $\delta^{18}\text{O}_P$  estimates from Lutz et al. (2018), which are based on raw observations from 24 precipitation collectors spread over the larger area of the Bode region. The spatial interpolation in Lutz et al. (2018) was conducted using kriging with altitude as an external drift. The kriged  $\delta^{18}\text{O}_P$  were further weighted with spatially distributed monthly precipitation to obtain representative estimates for the study region.

140 SAS model results are sensitive to the choice of the temporal resolution of input tracer data, and shorter time steps are generally recommended to achieve a satisfactory level of detail (Benettin and Bertuzzo, 2018). Additionally, a forward Euler scheme was employed to solve Eq. 2, whose precision increases with high frequency time steps. For this reason, we reconstructed daily  $\delta^{18}\text{O}_P$  estimates from monthly values with two different interpolation schemes. First, we used a step function in which the values between two consecutive samples assumed the value of the last sample. Second, we used a sine interpolation based on  
145 the assumption that the  $\delta^{18}\text{O}_P$  values follow a seasonal cycle (Fig. S1 in the Supplement, (Feng et al., 2009)), whose signature over a period of one year can be described by (Kirchner, 2016a):

$$\delta^{18}\text{O}_P(t) = a_P \cdot \cos(2 \cdot \pi \cdot f \cdot t) + b_P \cdot \sin(2 \cdot \pi \cdot f \cdot t) + k_P \quad (10)$$

where  $a$  and  $b$  are regression coefficients,  $t$  is the time (decimal years),  $f$  is the frequency ( $\text{yr}^{-1}$ ) and  $k$  ( $\%$ ) is the vertical offset of the isotope signal. The coefficients  $a$  and  $b$  were estimated by fitting Eq. 10 to monthly  $\delta^{18}\text{O}_P$  values using the iteratively  
150 re-weighted least squares (IRLS) estimation (von Freyberg et al., 2018). Subsequently, the estimated regression coefficients were used in Eq. 10 to obtain isotope data at daily frequency. Figure S2 in the Supplement displays the simulated kriged and raw  $\delta^{18}\text{O}_P$  values via step function and sine interpolation.

### 3.3 Estimation of the young water fraction ( $F_{yw}$ )

$F_{yw}$  was estimated through a sine-wave fit, which assumes that the seasonal cycle in  $\delta^{18}\text{O}_P$  is transmitted into  $\delta^{18}\text{O}_Q$  as a  
155 damped and phase-shifted signal (Soulsby et al., 2006). In line with (Bliss, 1970), the isotopic signal for  $\delta^{18}\text{O}_P$  and  $\delta^{18}\text{O}_Q$  over a year can be written respectively as (Kirchner, 2016a):

$$c_P(t) = A_P \cdot \sin(2 \cdot \pi \cdot f \cdot t - \phi_P) + k_P \quad (11)$$

$$c_Q(t) = A_Q \cdot \sin(2 \cdot \pi \cdot f \cdot t - \phi_Q) + k_Q \quad (12)$$

where  $A$  is the tracer cycle amplitude ( $\%$ ),  $\phi$  is the phase of the cycle (radians),  $t$  is the time (decimal years),  $f$  is the frequency  
160 ( $\text{yr}^{-1}$ ) and  $k$  ( $\%$ ) is the vertical offset of the isotope signal. The amplitude ratio defines the young water fraction  $F_{yw}$  (Kirchner, 2016a):

$$F_{yw}^{est} = \frac{A_Q}{A_P}. \quad (13)$$

$A_P$  and  $A_Q$  were calculated with the IRLS method by fitting Eqs. 11 and 12 to monthly  $\delta^{18}\text{O}_P$  and  $\delta^{18}\text{O}_Q$  samples volume-weighted with the corresponding  $P$  and  $Q$  rates; thus, the flow-weighted  $F_{yw}^{est}$  was computed (von Freyberg et al., 2018).  
165 Gaussian error propagation was applied to assess the standard error ( $\pm$  SE) of  $F_{yw}^{est}$  as an uncertainty measure.



This tracer-based  $F_{yw}^{est}$  was compared with the simulated young water fraction  $F_{yw}^{sim}$  obtained via the SAS model. To determine  $F_{yw}^{sim}$ , we averaged the TTDs computed at any time step; then, we flow-weighted the averaged TTDs to obtain the long-term TTD over the entire study period, also known as marginal TTD (Heidbüchel et al., 2012). From the marginal TTD, we computed  $F_{yw}^{sim}$  as:

$$170 \quad F_{yw}^{sim} = P_Q(T = \tau_{yw}). \quad (14)$$

where  $\tau_{yw}$  is the threshold age set to 75 days, which falls within 2-3 months defining  $F_{yw}$  (Kirchner, 2016a). We used  $F_{yw}^{est} \pm SE$  instead of a specific value to account for the uncertainty associated with a fixed threshold age of  $\tau_{yw}=75$  days for  $F_{yw}^{sim}$ .

### 3.4 Experimental design

In this study, different scenarios were used to quantify uncertainty in the modeled results. We tested twelve setups composed of three SAS functions (PLTI, PLTV, BETA), two temporal (step and sine function) and two spatial (raw and kriging values) interpolation techniques (Table 1). For each setup, we performed a Monte Carlo experiment by running the model with 10,000 parameter sets generated by the Latin Hypercube Sampling (LHS, McKay et al., 1979). Model parameters and their search ranges are shown in Table 2.

**Table 1.** List of model setups.

setup	interpolation	SAS function
1	step function kriged $\delta^{18}O_P$	PLTI
2		PLTV
3		BETA
4	step function raw $\delta^{18}O_P$	PLTI
5		PLTV
6		BETA
7	sine function kriged $\delta^{18}O_P$	PLTI
8		PLTV
9		BETA
10	sine function raw $\delta^{18}O_P$	PLTI
11		PLTV
12		BETA

**Table 2.** Model parameters and search ranges.

SAS parameter	Symbol	Unit	Lower Bound	Upper Bound
Discharge SAS parameter	$k_Q$	[-]	0.1	2
Discharge SAS parameter	$k_{Q1}$ or $\alpha$	[-]	0.1	2
Discharge SAS parameter	$k_{Q2}$ or $\beta$	[-]	0.1	2
Evapotranspiration SAS parameter	$k_{ET}$	[-]	0.1	2
Initial storage	$S_0$	[mm]	300	3000





A 5 years warm-up period (i.e., repetition of the input data) from February 2008 to January 2013 was performed to reduce the  
180 impact of the model initialization. The period from February 2013 to May 2015 was used to infer behavioral model parameters  
(i.e., parameter sets giving acceptable predictions), and subsequently to interpret the model results. The initial concentration of  
 $\delta^{18}\text{O}$  in storage was set to 9.2 ‰ coinciding with the mean  $\delta^{18}\text{O}_Q$  over the study period.

The generalized likelihood uncertainty estimation (GLUE Beven and Binley, 1992) was applied to determine the behavioral  
parameter sets in terms of the Kling-Gupta efficiency (KGE Gupta et al., 2009) for observed and simulated  $\delta^{18}\text{O}_Q$  values. The  
185 best 5% parameter sets were selected as behavioral, from which we constructed the 90% confidence intervals (CI) to refine  
limits of the behavioral solutions for every output variable. Instead of fixing a threshold limit based on KGE, we set the sample  
size to allow for comparability of the results across different model setups.

From the daily TTDs, we extracted the temporal evolution of the daily median transit time ( $\text{TT}_{50}$  (days), i.e., the time elapsed  
until 50% of the infiltrated water is transferred to the outflow (Sprenger et al., 2016)), and used it as a metric for the streamflow  
190 age. This was done because TTDs are typically skewed with long tails (Kirchner et al., 2001); hence, the median is often more  
suitable as it is less impacted by the poor identifiability of the older water components (Benettin et al., 2017).

In a final step, the behavioral parameter sets identified via GLUE were further constrained with  $F_{\text{yw}}^{\text{est}}$ ; the behavioral solu-  
tions providing  $F_{\text{yw}}^{\text{sim}}$  (Eq. 14) within the range  $F_{\text{yw}}^{\text{est}} \pm \text{SE}$  (Eq. 13) were chosen as the final behavioral solutions.

## 4 Results

### 195 4.1 Simulated $\delta^{18}\text{O}$ in streamflow and model performances

Modeled  $\delta^{18}\text{O}$  in streamflow ( $\delta^{18}\text{O}_Q$ ) represented by the 90% confidence interval (CI) in the ensemble solution are displayed  
in Fig. 2. The results reveal how the predicted  $\delta^{18}\text{O}_Q$  values enveloped the measured isotopic signature by reproducing its  
seasonal fluctuations, with depleted (i.e., more negative) values in winter and enriched (i.e., more positive) values in summer.  
However, the second half of the study period is characterized by more enriched predicted  $\delta^{18}\text{O}_Q$  values than the measured ones.  
200 Although the behavioral parameter sets are able to capture the seasonal isotopic trend, they poorly reproduced the exact values;  
therefore the ensemble simulations are characterized by a non-negligible uncertainty.

Figure 2 shows the distinct effects of the interpolated input tracer data and model parameterization on the simulated  $\delta^{18}\text{O}_Q$   
values. The step function interpolation generated an erratic isotopic signature in streamflow with flashy fluctuations, explicitly  
visible in Fig. 2c and f. On the other hand, the sine interpolation of  $\delta^{18}\text{O}_P$  values yielded a smooth response in the simulated  
205  $\delta^{18}\text{O}_Q$  values (Fig. 2g-l). Conversely, no clear visual difference was found between the raw (Fig. 2d-f and j-l) and kriged (Fig.  
2a-c and g-i)  $\delta^{18}\text{O}_P$  samples as their general patterns match (Fig. 2S in the Supplement). Likewise, distinct SAS parameteriza-  
tions produced remarkable differences in the simulated  $\delta^{18}\text{O}_Q$  values. BETA induced a large 90% CI in the  $\delta^{18}\text{O}_Q$  values (Fig.  
2c, f, i and l), and wide tracer cycle amplitudes. In contrast, both PLTI and PLTV (Fig. 2a, b, d, e, g, h, j and k) produced a  
substantially narrow 90% CI with small amplitudes of the simulated  $\delta^{18}\text{O}_Q$  values.

210 Despite the differences in the predicted  $\delta^{18}\text{O}_Q$  values, all simulations can be considered satisfactory given the KGE values  
ranging between 0.57 and 0.75, across all tested setups (Fig. 3). These performances can be classified from intermediate



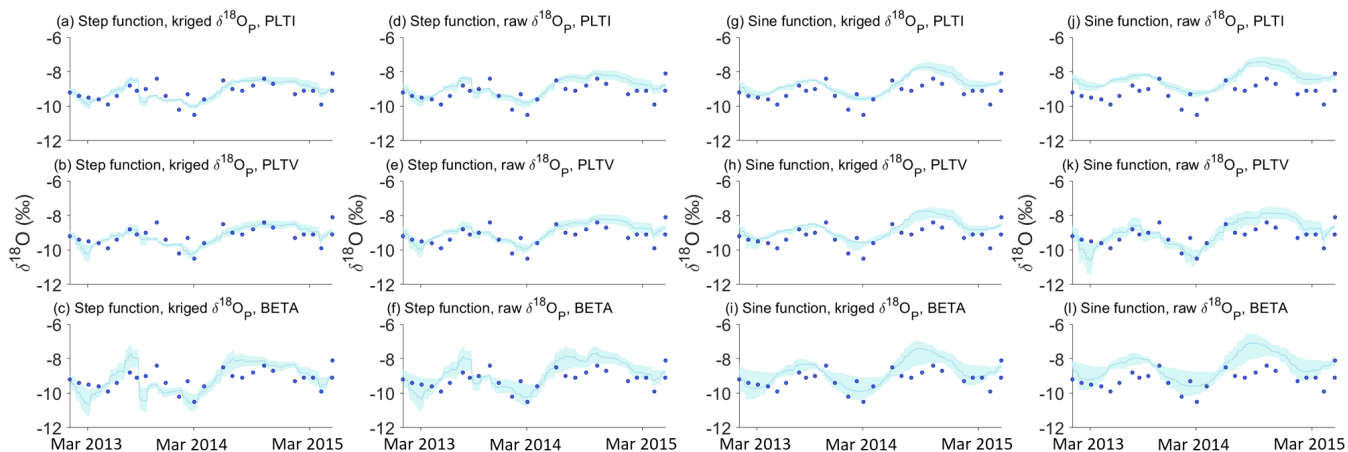


**Figure 2.** Predicted  $\delta^{18}\text{O}$  values in streamflow identified by 5% best KGE. Dark blue filled circles represent the observed data; the light blue line and the shaded area represent, respectively, the ensemble mean of all possible solutions and its variation range according to the 90% CI.

(Thiemig et al., 2013) to good (Andersson et al., 2017; Sutanudjaja et al., 2018). When considering the best fit, the combination of the step function interpolation and raw  $\delta^{18}\text{O}_p$  values performed best. Additionally, PLTV yielded slightly better KGE values than PLTI and BETA when grouping the setups with the same interpolation techniques of  $\delta^{18}\text{O}_p$ . Differences in the KGE means were statistically insignificant (t-test with p-values > 0.05) between setups 1 and 3, as well as among setups 6, 7 and 9 (Table 1), and this largely matches our visual analysis. Contrarily, the differences in the remaining setups were statistically significant (p-values < 0.05), indicating that a priori methodological choices (i.e., interpolation techniques of  $\delta^{18}\text{O}_p$  values and/or SAS parameterization) strongly impact on the overall results. Notwithstanding, this does not mean that we can clearly identify the most suitable setup .

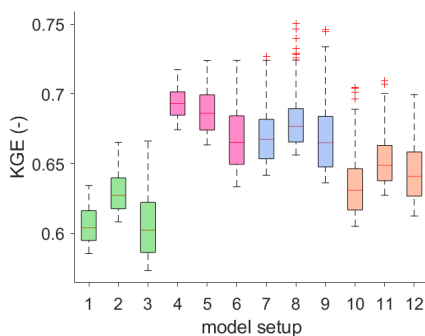


**Figure 3.** Boxplot of model performance ranges in behavioral solutions obtained with 5% best KGE; boxplots filled with the same colors represent model setups characterized by the same interpolation scheme in space and time. On each box, the central mark indicates the median, and the bottom and top edges of the box indicate the 25th and 75th percentiles, respectively. The whiskers extend to the most extreme data points not considered outliers, and the outliers are plotted individually using the '+' mark.



220 Ranges of the behavioral SAS parameters for the tested setups are summarized in Table S1 in the Supplement. Parameters  
for  $Q$  (i.e.,  $k_Q$ ,  $k_{Q1}$ ,  $k_{Q2}$ ,  $\alpha$  and  $\beta$ ) were different across the setups although, in general, they were relatively narrow and well  
identified. However, the behavioral parameters were better constrained when using the step function interpolation since their  
range was, on average, 34% narrower than that provided by the sine interpolation, across all the SAS parameterizations. The  
parameters  $k_{Q1}$  and  $\alpha$  were also better identified than  $k_{Q2}$  and  $\beta$ , since their range was, on average, 22% narrower, in all tested  
225 setups. Conversely, there was no significant difference in the parameters ranges when using kriged or raw  $\delta^{18}\text{O}_P$  values. The  
evapotranspiration parameter (i.e.,  $k_{ET}$ ) was poorly identified in all setups as any value in the search range provided equally  
good results. The initial storage  $S_0$  was only partially constrained as any value between 400 mm and 2340 mm was considered  
acceptable.

#### 4.2 Simulated transit times and model uncertainty

230 Figure 4 illustrates the 90% CI of the behavioral solutions for the predicted median transit times ( $\text{TT}_{50}$ ). The results show that  
the model simulates very different ranges of  $\text{TT}_{50}$  values based on the tested setups. When using PLTI and BETA, the 90%  
CI was relatively stable with small fluctuations throughout the simulation period, compared to PLTV (Fig. 4a, c, d, f, g, i, j  
and l). However, minor differences emerged across the simulated  $\text{TT}_{50}$ , as a result of the distinct interpolation techniques used  
for  $\delta^{18}\text{O}_P$  values. The 90% CI was on average slightly larger by 11%, across all tested setups, when using kriged  $\delta^{18}\text{O}_P$  (Fig.  
235 4a-c and g-i) rather than raw  $\delta^{18}\text{O}_P$  values (Fig. 4d-f and j-l). Also, the use of the sine function generated a 90% CI being on  
average 22% narrower across all tested setups, (Fig. 4g-l) with respect to the step function (Fig. 4a-f), notably within high flow  
conditions. In addition, the behavioral solutions obtained with BETA were more skewed towards shorter mean  $\text{TT}_{50}$  values,  
across all tested setups, in contrast to PLTI and PLTV (Fig. 4c, f, i and l).

Behavioral solutions obtained with PLTV revealed a similar pattern regardless of the interpolation employed (Fig. 4b, e, h  
240 and k). Nonetheless, there was a noticeable difference in the 90% CI under distinct flow regimes. During low flows and dry  
periods (i.e., late summer and autumn), the predicted  $\text{TT}_{50}$  show large uncertainties ranging at most between 286 and 895 days  
for the same moment in time (Fig. 4e). Conversely, during high flows (i.e., winter and spring), the 90% CI was narrow and  
varied at least between 135 and 163 days only (Fig. 4h). The large 90% CI and the notable differences across the tested setups  
highlight the sensitivity and, in turn, the uncertainty of predicted  $\text{TT}_{50}$  to the model parameterization, temporal interpolation  
245 of input data and hydrologic conditions. In contrast, the use of raw or kriged  $\delta^{18}\text{O}_P$  samples produced small differences in the  
estimated  $\text{TT}_{50}$ ; thus the spatial interpolation technique did not substantially affect the water age simulations.

In general, the variability of the predicted  $\text{TT}_{50}$  is controlled by the hydrological state of the system (Fig. 4). Discharge events  
reduced  $\text{TT}_{50}$  values, while low flow periods were associated with a longer estimated  $\text{TT}_{50}$ . This is expected as streamflow  
during high (low) flows is dominated by near-surface runoff (groundwater) with shallow (deep) flowpaths leading to a shorter  
250 (longer)  $\text{TT}_{50}$ . Such differences are particularly visible with PLTV (Fig. 4b, e, h, and k) as the exponent  $k_Q(t)$  shifts the water  
selection preference over time as a function of the wet/dry conditions; this makes the variability of  $\text{TT}_{50}$  more pronounced than  
that of PLTI and BETA, whose SAS parameters for  $Q$  are constant over time.

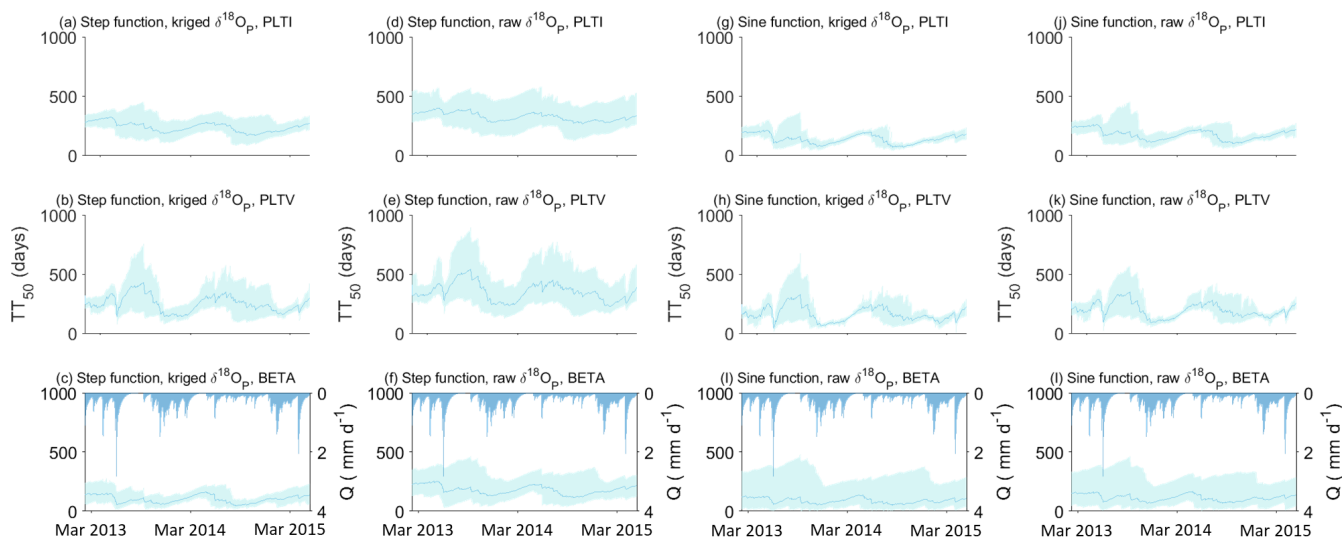


**Figure 4.** Predicted  $TT_{50}$  of streamflow identified by 5% best KGE; the light blue line and the shaded area represent, respectively, the ensemble mean of all possible solutions and its variation range according to the 90% CI.

### 4.3 Use of the young water fraction ( $F_{yw}$ )

The sine-wave fit produced young water fraction ( $F_{yw}^{est}$ ) values equal to  $0.25 \pm 0.08$  and  $0.22 \pm 0.07$  for kriged and raw  $\delta^{18}O_p$  samples, respectively. This means that approximately a quarter of the total streamflow is composed of water with ages younger than 2-3 months. Behavioral solutions produced SAS-based  $F_{yw}^{sim}$  values ranging between 0.22 and 0.54, across all tested setups, hence being much larger than  $F_{yw}^{est}$ . There were considerable differences in  $F_{yw}^{sim}$  across the SAS parameterizations as BETA produced a 37% larger  $F_{yw}^{sim}$  than that obtained with PLTI and PLTV, across the interpolation schemes. Moreover,  $F_{yw}^{sim}$  obtained with the sine interpolation was 31% larger than that of the step interpolation, across the tested setups. Conversely, no difference was found when using kriged or raw  $\delta^{18}O_p$  samples.

Figure 5 displays the simulated  $TT_{50}$  before (blue) and after (pink) using  $F_{yw}^{est}$  to reduce the uncertainty in the simulated  $TT_{50}$ . The results show that the addition of  $F_{yw}^{est}$  resulted in substantial changes in the 90% CI of  $TT_{50}$ , and the uncertainty reduction, in terms of percentage change, varied between 0% (Fig. 5b, d and e) and 49% (Fig. 5i) across the analysed setups. The lowest reduction occurred with the power law SAS functions and step function interpolation, with an average of 1% across the tested setups (Fig. 5a, b, d and e). In contrast, the 90% CI was largely reduced with BETA and the sine interpolation with an average of 42% across the setups (Fig. 5c, f, i and l). This clearly demonstrates the value of  $F_{yw}^{est}$  as an additional constraint in  $TT_{50}$  modelling.

### 4.4 Catchment-scale water release

SAS functions provided valuable insights into the catchment-scale water release dynamics. Figure 6 presents the behavioral solutions releasing water of different ages identified by 5% best KGE (blue) and after adding  $F_{yw}^{est}$  (pink), respectively.

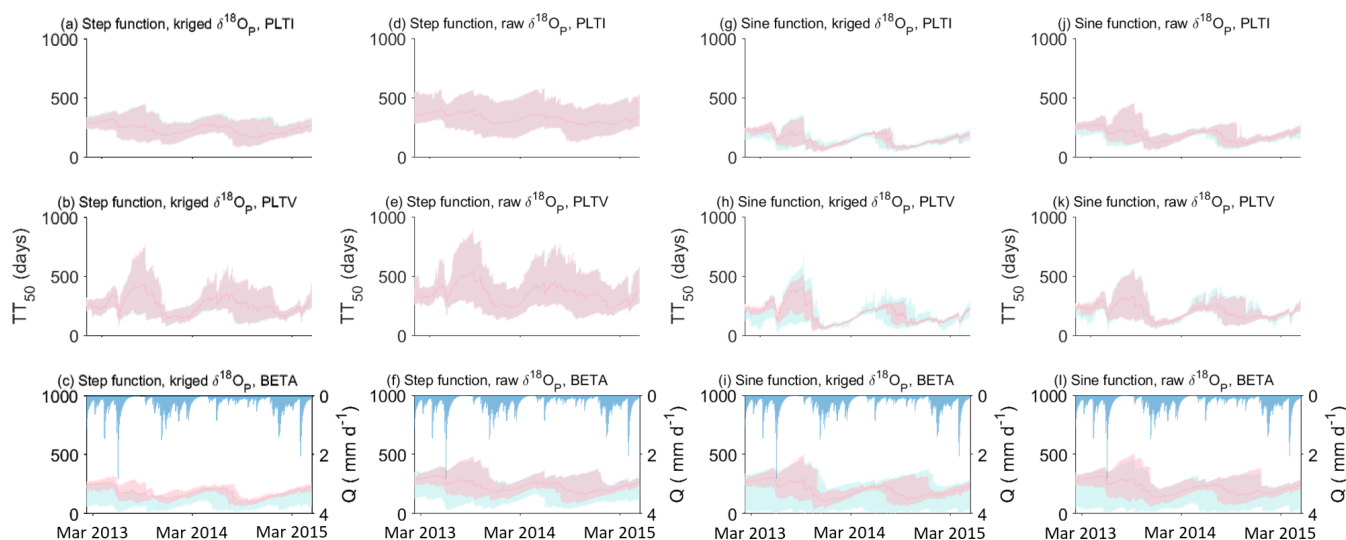


**Figure 5.** Predicted  $TT_{50}$  for streamflow identified by 5% best KGE (blue) and by adding  $F_{yw}^{est}$  (pink); the light blue (pink) line and the shaded area represent, respectively, the ensemble mean of all possible solutions and its variation range according to the 90% CI.

When considering the solutions identified by 5% best KGE, the catchment generally experienced a stronger affinity for young water (i.e.,  $k_Q < 1$ , or  $\alpha < 1$  and  $\beta > 1$ ), rather than old water (i.e.,  $k_Q > 1$ , or  $\alpha > 1$  and  $\beta < 1$ ). These findings are in agreement with other studies in the Upper Selke (Winter et al., 2020; Nguyen et al., 2021). Nonetheless, when PLTV is employed there is a considerable number of solutions indicating preference for both young and old water. Only a few solutions showed old water release, and this was 137% more prominent when using the sine interpolation and BETA, across all tested setups.

The use of  $F_{yw}^{est}$  as additional constraint drastically changed the water release scheme for some of the tested setups. Figure 6 shows that the catchment mainly released old water when using the sine interpolation (Fig. 6g and h), especially with PLTV and BETA. Although  $F_{yw}^{est}$  helped limit the uncertainty in the simulated  $TT_{50}$  under specific model assumptions,  $F_{yw}^{est}$  yielded contrasting results in the water release scheme, thus highlighting further sources of uncertainty related to those same setups.

## 280 5 Discussion

### 5.1 Uncertainty in TTD modelling

In this study we characterized the TTD uncertainty arising from model inputs (i.e., tracer data interpolated in time and space) and structure (i.e., SAS parameterizations). Our results show that the uncertainty (i.e., 90% CI) of the simulated  $TT_{50}$  was firmly dependent on the choice for the model setup (Fig. 4), and we found that the 90% CI was primarily sensitive to the SAS parameterizations as well as temporal interpolation of  $\delta^{18}O_p$ , rather than spatial interpolation of  $\delta^{18}O_p$ . Uncertainty in  $TT_{50}$  differed considerably between time-invariant (i.e. PLTI and BETA) and time-variant (i.e., PLTV) SAS functions. PLTI and BETA explicitly assume constant water selection preference over time, creating a moderately stable 90% CI with small

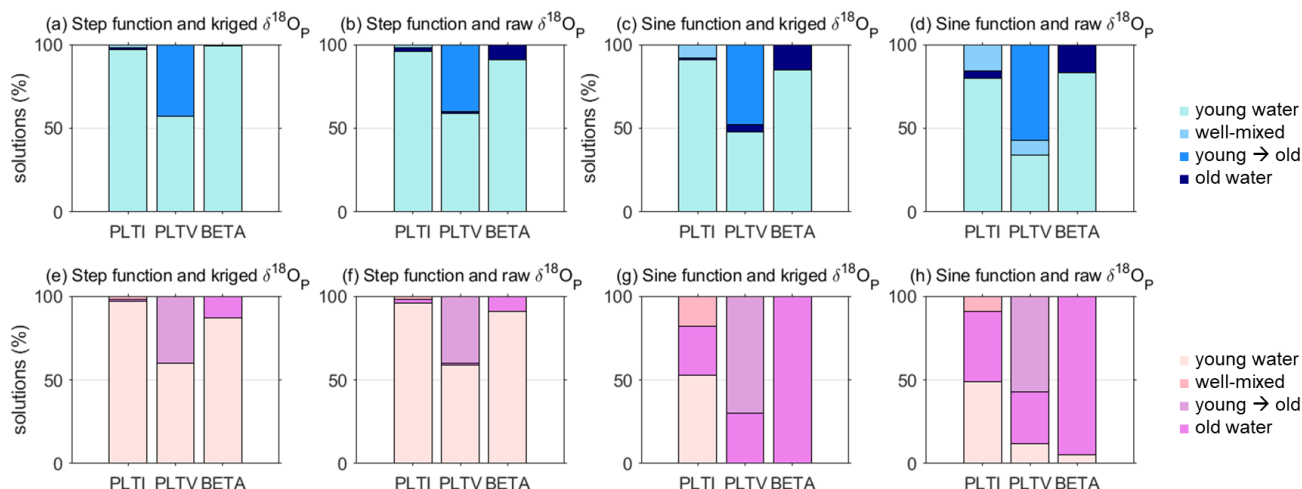


**Figure 6.** Percentage of behavioral solutions releasing water of different ages identified by 5% best KGE (blue) and by adding  $F_{yw}^{est}$  (pink).

fluctuations. Moreover, for these SAS functions, the 90% CI is biased towards the long-term average discharge behavior, which might prevent a correct representation of the full  $TT_{50}$  variability during precipitation events and droughts (Buzacott et al., 2020). However, PLTI and BETA could be appropriate where the catchment release scheme is expected to be relatively constant.

On the other hand, including an explicit time dependence strongly affected the 90% CI with respect to constant assumptions. PLTV produced a wider 90% CI, notably during low flow conditions, which can hinder the ability of the TTDs to provide robust insights on flow and solute transport. This highlights the need to constrain PLTV with further data. In addition, the exceptionally old flow components associated with a very large 90% CI might be a distortion of the actual  $TT_{50}$ , as they are known to be better estimated with reactive tracers rather than stable isotopes (Visser et al., 2019). Thus, PLTV-based  $TT_{50}$  that are greater than the observed period (828 days) should be interpreted carefully.

Despite the sizeable 90% CI, PLTV could be more capable of capturing the hillslope activation and deactivation of flowpaths driven by the precipitation regime (Angermann et al., 2017; Loritz et al., 2017). Also, PLTV could infer information on the time-variant water selection preference that could not be derived with PLTI and BETA. Indeed, PLTV showed the inverse storage effect, i.e., young water release during wet conditions rather than dry periods (Harman, 2015). This behavior may be the result of a rapid lateral transport due to rising water table (Pangle et al., 2017), and has been observed in many catchments (Benettin et al., 2017; Rodriguez et al., 2018; Wilusz et al., 2017, 2020).

Likewise, the high-frequency reconstruction of  $\delta^{18}O_P$  estimates from monthly values via interpolation created further uncertainty, as real data provide insights that are irreplaceable. The sine interpolation poorly reproduced heavily flashy rainfall events and only captured the average damped trend of the observed  $\delta^{18}O_P$  samples (Fig. S2 in the Supplement). Hence, related results must be interpreted with caution as tracer data uncertainty may conceal more pronounced transport processes (Dunn et al., 2008; Birkel et al., 2010; Hrachowitz et al., 2011). Contrarily, the step function interpolation preserved the maxima in



the monthly observed  $\delta^{18}\text{O}_P$  values, and reproduced their variation correctly. However, these results are based on this particular  
310 isotope dataset; the sine interpolation may be suitably applicable in other circumstances.

The dissimilarities in the simulated  $\text{TT}_{50}$  across the tested setups underline the importance of accounting for uncertainty in  
model-based TTDs. The uncertainty analysis performed in this study was essential to best describe the parameter identifiability  
and bounds of the behavioral solutions of each output variable. Furthermore, our results highlight the importance of gaining  
a good quality for tracer datasets and, possibly, employing the "true" model parameterization which correctly describes the  
315 catchment area. The second point can be defined according to a precise conceptual knowledge of the catchment's functioning  
(e.g., the geometry of the flow system) and information from previous studies in similar catchments.

## 5.2 On the value of young water fraction

The use of  $F_{yw}^{est}$  succeeded in limiting the uncertainty in the predicted  $\text{TT}_{50}$  obtained from the sine interpolation of  $\delta^{18}\text{O}_P$   
values and BETA. This reveals how these two setups combined are characterized by a high degree of uncertainty which  
320 is propagated into the simulated  $\text{TT}_{50}$ . We acknowledge that this is due to the sine interpolation, which only captured the  
average depleted trend of  $\delta^{18}\text{O}_P$  values (Fig. S2 in the Supplement). In addition, BETA is characterized by numerous behavioral  
solutions skewed towards short  $\text{TT}_{50}$  values and, in turn, large  $F_{yw}^{sim}$  (Fig. 4i and l), which might not correctly represent the  
 $\text{TT}_{50}$  values in the study area.

We recognize the robustness of  $F_{yw}^{est}$  obtained by the sine regression to ensure reliable  $\text{TT}_{50}$  values in this study. We  
325 attribute this to the moderately small standard errors in  $F_{yw}^{est}$  (0.07 and 0.08 for raw and kriged  $\delta^{18}\text{O}_P$  values, respectively).  
This is partly due to the fact that we used the same sampling period for  $\delta^{18}\text{O}$  in precipitation and streamflow, which limits  
the uncertainty of estimated  $F_{yw}^{est}$ . However, a higher temporal resolution of isotope samples rather than a coarser one could  
prevent bias toward smaller  $F_{yw}^{est}$  (Stockinger et al., 2016; Lutz et al., 2018). Also, to better represent the estimated  $F_{yw}^{est}$  from  
the sine regression, we could incorporate processes affecting the isotopic composition such as snowmelt (von Freyberg et al.,  
330 2018; Ceperley et al., 2020). Despite these limitations, based on our analysis, we acknowledge the potential of using  $F_{yw}^{est}$  for  
improving TTD predictions and limiting their uncertainty.

## 5.3 TTD modelling: advantages and limitations

Our results provide visually plausible seasonal fluctuations of the predicted  $\delta^{18}\text{O}_Q$  samples (Fig. 2), and satisfactory KGE  
values (Fig. 3), despite the uncertainty arising from both model inputs and structure. This corroborates our findings for the  
335 simulated  $\text{TT}_{50}$  in the Upper Selke. The magnitude of the uncertainty resulting from different setups cannot be generalized,  
but the overall approach for uncertainty assessment presented here could be extended to other areas and studies. However, we  
recognize some limitations and below indicate possible reasons and, in turn, improvements that future work could achieve.

First, the limited length of the  $\delta^{18}\text{O}$  timeseries might not describe the system accurately. Implementing longer timeseries  
could improve the parameter identifiability and provide a closer approximation of the TTDs. Second, this study relied only  
340 on stable water isotopes, which might underestimate the tails of the TTDs (Stewart et al., 2010; Seeger and Weiler, 2014).  
Possible advancements could be reached by using decaying tracers varying over a larger timescale than stable water isotopes





(e.g., tritium, (Stewart et al., 2012; Morgenstern et al., 2015)), and imparting more information on old water. Next, future work should retrieve more information on  $ET$  and the initial storage  $S_0$ , whose parameters were poorly identified. However, this issue is common in transport studies that rely on measurements of instream stable water isotope (Benettin et al., 2017; Buzacott et al., 2020). As a way forward, information on the  $ET$  isotopic compositions might help better constrain  $ETET$  parameters and assess their affinity for young/old water. Regarding constraining the range of  $S_0$ , further information can be gained knowing the geophysical properties of catchment (i.e., geological structure and physical characteristics) (Holbrook et al., 2014), and using decaying isotopes (Visser et al., 2019). Finally, future research should better explore the validity of  $F_{yw}$  to limit the predictive uncertainty in TTDs, by exploring whether the effectiveness of  $F_{yw}$  for TTD estimation depends on catchment's attributes (e.g., size, annual precipitation, flow rates, soil and vegetation).

#### 5.4 Implications of TTD uncertainties

This study characterized the uncertainty in TTDs, which summarize the catchment's hydrologic transport behavior, thereby comprise decisive information for water managers. The uncertainty in the predicted  $TT_{50}$  has relevant implications for both water quantity and quality; the larger the 90% CI in the simulated  $TT_{50}$ , the greater the difference in the  $TT_{50}$  values, which, ultimately, implies distinct water release and solute export dynamics (McDonnel et al., 2010).

Uncertainty in TTDs may be crucial for characterizing the catchment's response to climatic changes (Wilusz et al., 2017). Considering the increasing severity of droughts (Dai, 2013), a catchment that largely releases young water might be more affected by droughts than a catchment whose stream is fed by relatively old water sources. A short  $TT_{50}$  reveals a low drought resilience of the catchment, which could limit streamflow generation processes and change the instream water quality status. Likewise, TTD uncertainty may affect the quantification of the modern groundwater age, i.e., groundwater younger than 50 years (Bethke and Johnson, 2008). According to (Jasecko, 2019), the correct identification of modern groundwater abundance and distribution can help determine its renewal (Le Gal La Salle et al., 2001; Huang et al., 2017), wells and depths most likely to contain contaminants (Visser et al., 2013; Opazo et al., 2016), and the part of the aquifer flushed more rapidly.

Uncertainty in TTDs also impacts on the fate of dissolved solutes, such as nitrates (Yang, X. et al., 2018; Nguyen et al., 2021), pesticides (Holvoet et al., 2007; Lutz et al., 2017), and chlorides (Kirchner et al., 2000; Benettin et al., 2013). These solutes constitute a crucial source of diffuse water pollution in agricultural areas (Jiang et al., 2014; Kumar et al., 2020), as they are spread on the soil during the fertilization period. Exposure time of nitrates with the soil matrix has strong consequences for biogeochemical reactions, such as denitrification (Kolbe et al., 2019; Kumar et al., 2020). A short  $TT_{50}$  suggests that water can be rapidly conveyed to the stream network (Kirchner et al., 2001), with limited time for denitrification. This explains the elevated instream concentration and short-term impact of nitrate export compared to that of a longer  $TT_{50}$ , which is typically associated with old water release and low nitrate concentration (Nguyen et al., 2021). Similarly, pesticide transport is highly affected by the TTD uncertainty as a long  $TT_{50}$  may decelerate pesticide degradation due to decreased microbial activity along deeper flowpaths (Rodríguez-Cruz et al., 2006). In other cases, a shorter  $TT_{50}$  may limit the time for degradation causing a peak in the instream concentration (Leu et al., 2004). Overall, a longer  $TT_{50}$  can delay or buffer the catchment's reactive solute response at the outlet (Dupas et al., 2016; Van Meter et al., 2017). This creates a long-term effect of hydrological legacies and





a continuous problem with diffuse pollution of nitrates (Ehrhardt et al., 2019; Winter et al., 2020) and pesticides (Lutz et al., 2013), which can persist in the catchment for several years. Finally, TTD uncertainties also play an important role in chloride transport, although chlorides are commonly known to be conservative (Svensson et al., 2012). A short  $TT_{50}$  may indicate rapid chloride mobilization, whereas a long  $TT_{50}$  implies chloride persistence in groundwater; thereby chloride accumulates and is released at lower rates, with impacts on the ecosystem functions, vegetation uptake and metabolism (Xu et al., 1999).

Understanding the uncertainty in TTDs is crucial for the aforementioned implications. In this study, we want to convey that it is essential to characterize the specific sources of uncertainty, which can stem from model inputs, structure and parameters, as well as their combined effects on the predicted TTDs. Uncertainty is omnipresent in TTD-based modeling, and we need to recognise it, especially when dealing with sparse tracer data and multiple choices for model parameterization, which affect the calculated  $TT_{50}$ . We also acknowledge the potential of incorporating additional information on water ages based on  $F_{yw}$ , which has contributed to reduce  $TT_{50}$  uncertainties.

## 6 Conclusions

This study explored the uncertainty in TTDs of streamflow, resulting from twelve model setups obtained from different SAS parameterizations (i.e., PLTI, PLTV and BETA), and reconstruction of the precipitation isotopic signature in time and space via interpolation (step function vs. sine-fit, raw vs. kriged values).

We found satisfactory KGE values, whose differences across the tested setups were statistically significant, meaning that the choice of the setup matters and, as a consequence, distinct setups led to considerably different simulated  $TT_{50}$  values. The choice between using time-variant or time-invariant SAS functions was crucial as the time-invariant SAS function generated a bias in the estimated  $TT_{50}$  toward the long-term average discharge behavior, which might be appropriate for catchments experiencing smooth changes in the hydrologic conditions. On the other hand, the time-variant SAS function captured the dynamics of the catchment wetness, resulting in very high seasonality of  $TT_{50}$ . However, the time-variant SAS function also produced a larger 90% CI, which indicates the need to constrain the function with additional data. Results from the temporal interpolation using a sine curve must be interpreted carefully as they poorly reproduced flashy events in precipitation, thus indicating that some more dynamic transport processes were not fully accounted for. Conversely, the step function interpolation was able to intercept the measured  $\delta^{18}O_p$  data. Dry conditions were another reason for uncertainty as indicated by the high variance in the simulated  $TT_{50}$  values. Finally, the use of  $F_{yw}$  as an additional constraint was promising in reducing  $TT_{50}$  uncertainties, particularly when using the sine interpolation of  $\delta^{18}O_p$  samples combined with BETA.

Our study provides new insights into the TTDs uncertainty when high-frequency tracer data are missing and the SAS framework is used. Regardless of the degree of efficiency or uncertainty, the decision on which setup is more plausible depends on a full conceptual knowledge of the catchment functioning. We consider the presented approach as potentially applicable to other studies for enabling a better characterization of TTDs uncertainty, improving TTD simulations and, ultimately, informing water management. These aspects are particularly crucial in view of evermore extreme climatic conditions and increasing water pollution under global change.



410 *Code and data availability.* The model used in this study is presented at <https://doi.org/10.5194/gmd-11-1627-2018>. The iteratively re-weighted least squares (IRLS) method used to get modelled daily kriged and raw isotope ( $\delta^{18}\text{O}$ ) in precipitation with the sine interpolation, as well as the estimated young water fraction ( $F_{yw}$ ), is presented at <https://doi.org/10.5194/hess-22-3841-2018>. Hydroclimatic timeseries,  $\delta^{18}\text{O}$  data and interpolated  $\delta^{18}\text{O}$  timeseries can be accessed at <https://zenodo.org/record/6630477#.YqL7wBpBxaQ>.

415 *Author contributions.* AB conducted the model simulations, the analysis and interpretation of the results, and wrote the original draft of the paper. SRL and RK designed and conceptualized the study, and provided data for model simulations. TVN provided technical support for modeling and helped organize the structure and content of the paper. AB, SRL, RK and TVN conceived the methodology and experimental design. All co-authors helped AB interpret the results. All authors contributed to the review, final writing and finalization of this work.

*Competing interests.* RK is a member of the editorial board of Hydrology and Earth System Sciences.



## References

- Ajami, N. K., Duan, Q., and Sorooshian, S.: An integrated hydrologic Bayesian multimodel combination framework: Con-  
420 fronting input, parameter, and model structural uncertainty in hydrologic prediction, *Water Resour. Res.*, 43, W01403,  
<https://doi.org/10.1029/2005WR004745>, 2007.
- Andersson, J. C. M., Arheimer, B., Traoré, F., Gustafsson, D., , and Ali, A.: Process refinements improve a hydrological model concept  
applied to the Niger River basin, *Hydrol. Process.*, 31, 4540–4554, <https://doi.org/10.1002/hyp.11376>, 2017.
- Angermann, L., Jackisch, C., Allroggen, N., Sprenger, M., Zehe, E., Tronicke, J., Wiler, M., and Blume, T.: Form and function in  
425 hillslope hydrology: characterization of subsurface flow based on response observations, *Hydrol. Earth Syst. Sci.*, 21, 3727–3748,  
<https://doi.org/10.5194/hess-21-3727-2017>, 2017.
- Asadollahi, M., Stumpp, C., Rinaldo, A., and Benettin, P.: Transport and water age dynamics in soils: A comparative study of spatially  
integrated and spatially explicit models, *Water Resour. Res.*, 56, e2019WR025539, <https://doi.org/10.1029/2019WR025539>, 2020.
- Benettin, P. and Bertuzzo, E.: tran-SAS v1.0: a numerical model to compute catchment-scale hydrologic transport using StorAge Selection  
430 functions, *Geosci. Model Dev.*, 11, 1627–1639, <https://doi.org/10.5194/gmd-11-1627-2018>, 2018.
- Benettin, P., van der Velde, Y., van der Zee, S. E. A. T. M., Rinaldo, A., and Botter, G.: Chloride circulation in a lowland catchment and the  
formulation of transport by travel time distributions, *Water Resour. Res.*, 49, 4619–4632, <https://doi.org/10.1002/wrcr.20309>, 2013.
- Benettin, P., Bailey, S. W., Campbell, J. L., Green, M. B., Rinaldo, A., Likens, G. E., J., M. K., and Botter, G.: Linking water age  
and solute dynamics in streamflow at the Hubbard Brook Experimental Forest, NH, USA, *Water Resour. Res.*, 51, 9256–9272,  
435 <https://doi.org/10.1002/2015WR017552>, 2015a.
- Benettin, P., Kirchner, J. W., Rinaldo, A., and Botter, G.: Modeling chloride transport using travel time distributions at Plynlimon, Wales,  
*Water Resour. Res.*, 51, 3259–3276, <https://doi.org/10.1002/2014WR016600>, 2015b.
- Benettin, P., Soulsby, C., Birkel, C., Tetzlaff, D., Botter, G., and Rinaldo, A.: Using SAS functions and high-resolution isotope data to unravel  
travel time distributions in headwater catchments, *Water Resour. Res.*, 53, 1864–1878, <https://doi.org/10.1002/2016WR020117>, 2017.
- 440 Bethke, C. M. and Johnson, T. M.: Groundwater age and groundwater age dating, *Annu. Rev. Earth Planet. Sci.*, 36, 121–152,  
<https://doi.org/10.1146/annurev.earth.36.031207.124210>, 2008.
- Beven, K.: A manifesto for the equifinality thesis, *J. Hydrol.*, 320, 18–36, <https://doi.org/10.1016/j.jhydrol.2005.07.007>, 2006.
- Beven, K. and Binley, A.: The future of distributed models: model calibration and uncertainty prediction, *Hydrol. Process.*, 6, 279–298,  
<https://doi.org/10.1002/hyp.3360060305>, 1992.
- 445 Beven, K. and Freer, J.: Equifinality, data assimilation, and uncertainty estimation in mechanistic modelling of complex environmental  
systems using the GLUE methodology, *J. Hydrol.*, 249, 11–29, [https://doi.org/10.1016/S0022-1694\(01\)00421-8](https://doi.org/10.1016/S0022-1694(01)00421-8), 2001.
- Birkel, C. and Soulsby, C.: Advancing tracer-aided rainfall-runoff modelling: A review of progress, problems and unrealised potential,  
*Hydrol. Process.*, 29, 5227–5240, <https://doi.org/10.1002/hyp.10594>, 2015.
- Birkel, C., Dunn, S. M., Tetzlaff, D., and Soulsby, C.: Assessing the value of high-resolution isotope tracer data in the stepwise development  
450 of a lumped conceptual rainfall–runoff model, *Hydrol. Process.*, 24, 2335–2348, <https://doi.org/10.1002/hyp.7763>, 2010.
- Bliss, C. I.: *Statistics in biology: Statistical methods for research in the natural sciences* (Vol. 2), New York: McGraw-Hill,  
<https://doi.org/10.1002/bimj.19690110327>, 1970.
- Botter, G., Bertuzzo, E., Bellin, A., and Rinaldo, A.: On the Lagrangian formulations of reactive solute transport in the hydrologic response,  
*Water Resour. Res.*, 41, W04008, <https://doi.org/10.1029/2004WR003544>, 2005.



- 455 Botter, G., Bertuzzo, E., and Rinaldo, A.: Transport in the hydrologic response: Travel time distributions, soil moisture dynamics, and the old water paradox, *Water Resour. Res.*, 46, W03 514, <https://doi.org/10.1029/2009WR008371>, 2010.
- Botter, G., Bertuzzo, E., and Rinaldo, A.: Catchment residence and travel time distributions: The master equation, *Geophys. Res. Lett.*, 38, L11 403, <https://doi.org/10.1029/2011GL047666>, 2011.
- Buzacott, A. J. V., van der Velde, Y., Keitel, C., and Vervoort, R. W.: Constraining water age dynamics in a south-eastern Australian catchment using an age-ranked storage and stable isotope approach, *Hydrol. Process.*, 34, 4384–4403, <https://doi.org/10.1002/hyp.13880>, 2020.
- 460 Ceperley, N. Zuecco, G., Beria, H., Carturan, L., Michelon, A., Penna, D., Larsen, J., and Schaeffli, B.: Seasonal snow cover decreases young water fractions in high Alpine catchments, *Hydrol. Process.*, 34, 4794–4813, <https://doi.org/10.1002/hyp.13937>, 2020.
- Dai, A.: Erratum: Increasing drought under global warming in observations and models, *Nature Clim Change*, 3, 171, <https://doi.org/10.1038/nclimate1811>, 2013.
- 465 Danesh-Yazdi, M., Foufoula-Georgiou, E., Karwan, D. L., and Botter, G.: Inferring changes in water cycle dynamics of intensively managed landscapes via the theory of time-variant travel time distributions, *Water Resour. Res.*, 52, 7593–7614, <https://doi.org/10.1002/2016WR019091>, 2016.
- Danesh-Yazdi, M., Klaus, J., Condon, L. E., and Maxwell, R. M.: Bridging the gap between numerical solutions of travel time distributions and analytical storage selection functions, *Hydrol. Process.*, 32, 1063–1076, <https://doi.org/10.1002/hyp.11481>, 2018.
- 470 Yang, J., Heidbüchel, I., Musolff, A., Reinstorf, F., and Fleckenstein, J. H.: Exploring the Dynamics of Transit Times and Subsurface Mixing in a Small Agricultural Catchment, *Water Resour. Res.*, 54, 2317–2335, <https://doi.org/10.1002/2017WR021896>, 2018.
- Yang, X., Seifeddine, J., Zink, M., Fleckenstein, J. H., Borchardt, D., and Rode, M.: A New Fully Distributed Model of Nitrate Transport and Removal at Catchment Scale, *Water Resour. Res.*, 54, 5856–5877, <https://doi.org/10.1029/2017WR022380>, 2018.
- Drever, M. C. and Hrachowitz, M.: Migration as flow: using hydrological concepts to estimate the residence time of migrating birds from the daily counts, *Methods Ecol. Evol.*, 8, 1146–1157, <https://doi.org/10.1111/2041-210X.12727>, 2017.
- 475 Dunn, S. M., Bacon, J. R., Soulsby, C., Tetzlaff, D., Stutter, M. I., Waldron, S., and Malcolm, I. A.: Interpretation of homogeneity in  $\delta^{18}\text{O}$  signatures of stream water in a nested sub-catchment system in north-east Scotland, *Hydrol. Process.*, 22, 4767–4782, <https://doi.org/10.1002/hyp.7088>, 2008.
- Dupas, R., Jomaa, S., Musolff, A., Borchardt, D., and Rode, M.: Disentangling the influence of hydroclimatic patterns and agricultural management on river nitrate dynamics from sub-hourly to decadal time scales, *Sci. Total Environ.*, 571, 791–800, <https://doi.org/10.1016/j.scitotenv.2016.07.053>, 2016.
- 480 Dupas, R., Musolff, A., Jawitz, J. W., Rao, P. S. C., Jäger, C. G., Fleckenstein, J. H., Rode, M., and Borchardt, D.: Carbon and nutrient export regimes from headwater catchments to downstream reaches, *Biogeosciences*, 14, 4391–4407, <https://doi.org/10.5194/bg-14-4391-2017>, 2017.
- 485 Duvert, C., Stewart, M. K., Cendon, D. I., and Raiber, M.: Time series of tritium, stable isotopes and chloride reveal short-term variations in groundwater contribution to a stream, *Hydrol. Earth Syst. Sci.*, 20, 257–277, <https://doi.org/10.5194/hess-20-257-2016>, 2016.
- Ehrhardt, S., Kumar, R., Fleckenstein, J. H., Attinger, S., and Musolff, A.: Trajectories of nitrate input and output in three nested catchments along a land use gradient, *Hydrol. Earth Syst. Sci.*, 23, 3503–3524, <https://doi.org/10.5194/hess-23-3503-2019>, 2019.
- Feng, X., Faiia, A. M., and Posmentier, E. S.: Seasonality of isotopes in precipitation: A global perspective, *J. Geophys. Res.*, 114, D08 116, <https://doi.org/10.1029/2008jd011279>, 2009.
- 490 Gupta, H. V., Kling, H., Yilmaz, K. K., and Martinez, G. F.: Decomposition of the mean squared error and NSE performance criteria: Implications for improving hydrological modelling, *J. Hydrol.*, 377, 80–91, <https://doi.org/10.1016/j.jhydrol.2009.08.003>, 2009.



- Harman, C. J.: Time-variable transit time distributions and transport: Theory and application to storage-dependent transport of chloride in a watershed, *Water Resour. Res.*, 51, 1–30, <https://doi.org/10.1002/2014WR015707>, 2015.
- 495 Harman, C. J.: Age-Ranked Storage-Discharge Relations: A Unified Description of Spatially Lumped Flow and Water Age in Hydrologic Systems, *Water Resour. Res.*, 55, 7143–7165, <https://doi.org/10.1029/2017WR022304>, 2019.
- Heidbüchel, I., Yang, J., Musolff, A., Troch, P., Ferré, T., and Fleckenstein, J. H.: On the shape of forward transit time distributions in low-order catchments, *Hydrol. Earth Syst. Sci.*, 24, 2895–2920, <https://doi.org/10.5194/hess-24-2895-2020>, 2020.
- Heidbüchel, I., Troch, P. A., Lyon, S. W., and Wiler, M.: The master transit time distribution of variable flow systems, *Water Resour. Res.*, 500 48, W06520, <https://doi.org/10.1029/2011WR011293>, 2012.
- Holbrook, W. S., Riebe, C. S., Elwaseif, M., Hayes, J. L., Basler-Reeder, K., Harry, D. L., Malazian, A., Dosseto, A., Hartsough, P. C., and Hopmans, J. W.: Geophysical constraints on deep weathering and water storage potential in the Southern Sierra Critical Zone Observatory, *Earth Surface Processes and Landforms*, 39, 366–380, <https://doi.org/10.1002/esp.3502>, 2014.
- Holvoet, K. M., Seuntjens, P., and Vanrolleghem, P. A.: Monitoring and modeling pesticide fate in surface waters at the catchment scale, 505 *Ecol. Model.*, 209, 53–64, <https://doi.org/10.1016/j.ecolmodel.2007.07.030>, 2007.
- Hrachowitz, M., Soulsby, C., Tetzlaff, D., Malcolm, I. A., and Schoups, G.: Gamma distribution models for transit time estimation in catchments: Physical interpretation of parameters and implications for time-variant transit time assessment, *Water Resour. Res.*, 46, W10536, <https://doi.org/10.1029/2010WR009148>, 2010.
- Hrachowitz, M., Soulsby, C., Tetzlaff, D., and Malcolm, I. A.: Sensitivity of mean transit time estimates to model conditioning and data 510 availability, *Hydrol. Process.*, 25, 980–990, <https://doi.org/10.1002/hyp.7922>, 2011.
- Hrachowitz, M., Savenije, H., Bogaard, T. A., Tetzlaff, D., and Soulsby, C.: What can flux tracking teach us about water age distribution patterns and their temporal dynamics?, *Hydrol. Earth Syst. Sci.*, 17, 533–564, <https://doi.org/10.5194/hess-17-533-2013>, 2013.
- Hrachowitz, M., Benettin, P., van Breukelen, B. M., Fovet, O., Howden, N. J. K., Ruiz, L van der Velde, Y., and Wade, A. J.: Transit times — the link between hydrology and water quality at the catchment scale, *WIREs Water*, 3, 629–657, <https://doi.org/10.1002/wat2.1155>, 2016.
- 515 Huang, T., Pang, Z., Li, J., Xiang, Y., and Zhao, Z.: Mapping groundwater renewability using age data in the Baiyang alluvial fan, NW, China, *Hydrogeol J.*, 25, 743–755, <https://doi.org/10.1007/s10040-017-1534-z>, 2017.
- Jasecko, S.: Global isotope hydrogeology — review, *Reviews of Geophysics*, 57, 835–965, <https://doi.org/10.1029/2018RG000627>, 2019.
- Jiang, S., Jomaa, S., and Rode, M.: Modelling inorganic nitrogen leaching in nested mesoscale catchments in central Germany, *Ecohydrol.*, 7, 1345–1362, <https://doi.org/10.1002/eco.1462>, 2014.
- 520 Jing, M., Heße, F., Kumar, R., Kolditz, O., Kalbacher, T., and Attinger, S.: Influence of input and parameter uncertainty on the prediction of catchment-scale groundwater travel time distributions, *Hydrol. Earth Syst. Sci.*, 23, 171–190, <https://doi.org/10.5194/hess-23-171-2019>, 2019.
- Kim, M., Pangle, L. A., Cardoso, C., Lora, M., Volkmann, T. H. M., Wang, Y., Harman, C. J., and Troch, P. A.: Transit time distributions and StorAge Selection functions in a sloping soil lysimeter with time-varying flow paths: Direct observation of internal and external transport 525 variability, *Water Resour. Res.*, 52, 7105–7129, <https://doi.org/10.1002/2016WR018620>, 2016.
- Kirchner, J. W.: Getting the right answers for the right reasons: Linking measurements, analyses, and models to advance the science of hydrology, *Water Resour. Res.*, 42, W03S04, <https://doi.org/10.1029/2005WR004362>, 2006.
- Kirchner, J. W.: Aggregation in environmental systems – Part 1: Seasonal tracer cycles quantify young water fractions, but not mean transit times, in spatially heterogeneous catchments, *Hydrol. Earth Syst. Sci.*, 20, 279–297, <https://doi.org/10.5194/hess-20-279-2016>, 2016a.



- 530 Kirchner, J. W.: Aggregation in environmental systems – Part 2: Catchment mean transit times and young water fractions under hydrologic nonstationarity, *Hydrol. Earth Syst. Sci.*, 20, 299–328, <https://doi.org/10.5194/hess-20-299-2016>, 2016b.
- Kirchner, J. W., Feng, X., and Neal, C.: Fractal stream chemistry and its implications for contaminant transport in catchments, *Nature*, 403, 524–527, <https://doi.org/10.1038/35000537>, 2000.
- Kirchner, J. W., Feng, X., and Neal, C.: Catchment-scale advection and dispersion as a mechanism for fractal scaling in stream tracer concentrations, *J. Hydrol.*, 254, 82–101, [https://doi.org/10.1016/S0022-1694\(01\)00487-5](https://doi.org/10.1016/S0022-1694(01)00487-5), 2001.
- 535 Kirchner, J. W., Feng, X., Neal, C., and Robson, A. J.: The fine structure of water-quality dynamics: the (high-frequency) wave of the future, *Hydrol. Process.*, 18, 1353–1359, <https://doi.org/10.1002/hyp.5537>, 2004.
- Kolbe, T., de Dreuzy, J. R., Abbott, B. W., Aquilina, L., Babey, T., Green, C. T., et al.: Stratification of reactivity determines nitrate removal in groundwater, *Proceedings of the National Academy of Sciences*, 116(7), 2494–2499, <https://doi.org/10.1073/pnas.1816892116>, 2019.
- 540 Kumar, R., Samaniego, L., and Attinger, S.: Implications of distributed hydrologic model parameterization on water fluxes at multiple scales and locations, *Water Resour. Res.*, 49, 360–379, <https://doi.org/10.1029/2012WR012195>, 2013.
- Kumar, R., Heße, F., Rao, P. S. C., Musolff, A., Jawitz, J. W., Sarrazin, F., Samaniego, L., Fleckenstein, J. H., Rakovec, O., Thober, S., and Attinger, S.: Strong hydroclimatic controls on vulnerability to subsurface nitrate contamination across Europe, *Nature Communications*, 11, 6302, <https://doi.org/10.1038/s41467-020-19955-8>, 2020.
- 545 Le Gal La Salle, C., Marlin, C., Leduc, C., Taupin, J. D., Massault, M., and Favreau, G.: Renewal rate estimation of groundwater based on radioactive tracers (<sup>3</sup>H, <sup>14</sup>C) in an unconfined aquifer in a semi-arid area, Iullemeden Basin, Niger, *J. Hydrol.*, 254, 145–156, [https://doi.org/10.1016/S0022-1694\(01\)00491-7](https://doi.org/10.1016/S0022-1694(01)00491-7), 2001.
- Leu, C., Singer, H., Stamm, C., Muller, S. R., and Schwarzenbach, R. P.: Simultaneous Assessment of Sources, Processes, and Factors Influencing Herbicide Losses to Surface Waters in a Small Agricultural Catchment, *Environ. Sci. Technol.*, 38, 3827–3834, <https://doi.org/10.1021/es0499602>, 2004.
- 550 Loritz, R., Hassler, S. K., Jackisch, C., Allroggen, N., van Schaik, L., Wienhöfer, J., and Zehe, E.: Picturing and modeling catchments by representative hillslopes, *Hydrol. Earth Syst. Sci.*, 21, 1225–1249, <https://doi.org/10.5194/hess-21-1225-2017>, 2017.
- Lutz, S., van Meerveld, H. J., Waterloo, M. J., Broers, H. P., and van Breukelen B. M.: A model-based assessment of the potential use of compound-specific stable isotope analysis in river monitoring of diffuse pesticide pollution, *Hydrol. Earth Syst. Sci.*, 17, 4505–4524, <https://doi.org/10.5194/hess-17-4505-2013>, 2013.
- 555 Lutz, S. R., van der Velde, Y., Elsayed, O. F., Imfeld, G., Lefrancq, M., Payraudeau, S., and van Breukelen, B. M.: Pesticide fate on catchment scale: conceptual modelling of stream CSIA data, *Hydrol. Earth Syst. Sci.*, 21, 5243–5261, <https://doi.org/10.5194/hess-21-5243-2017>, 2017.
- Lutz, S. R., Krieg, R., Müller, C., Zink, M., Knöller, K., Samaniego, L., and Merz, R.: Spatial patterns of water age: using young water fractions to improve the characterization of transit times in contrasting catchments, *Water Resour. Res.*, 54, 4767–4784, <https://doi.org/10.1029/2017WR022216>, 2018.
- McDonnel, J. J., McGuire, K., Aggarwal, P., Beven, K. J., Biondi, D., Destouni, G., et al.: How old is streamwater? Open questions in catchment transit time conceptualization, modelling and analysis, *Hydrol. Process.*, 24, 1745–1754, <https://doi.org/10.1002/hyp.7796>, 2010.
- 560 McGuire, K. J. and McDonnel, J. J.: A review and evaluation of catchment transit time modeling, *J. Hydrol.*, 330, 543–563, <https://doi.org/10.1016/j.jhydrol.2006.04.020>, 2006.



- McKay, M. D., Beckman, R. J., and Conover, W. J.: A Comparison of Three Methods for Selecting Values of Input Variables in the Analysis of Output from a Computer Code, *Technometrics*, 21, 239–245, <https://doi.org/10.2307/1268522>, 1979.
- 570 Morgenstern, U., Daughney, C. J., Leonard, G., Gordon, D., Donath, F. M., and Reeves, R.: Using groundwater age and hydrochemistry to understand sources and dynamics of nutrient contamination through the catchment into Lake Rotorua, New Zealand, *Hydrol. Earth Syst. Sci.*, 19, 803–822, <https://doi.org/10.5194/hess-19-803-2015>, 2015.
- Nguyen, T. V., Kumar, R., Lutz, S. R., Musloff, A., Yang, J., and Fleckenstein, J. H.: Modeling Nitrate Export From a Mesoscale Catchment Using StorAge Selection Functions, *Water Resour. Res.*, 57, e2020WR028490, <https://doi.org/10.1029/2020WR028490>, 2021.
- 575 Niemi, A. J.: Residence time distributions of variable flow processes, *The International Journal of Applied Radiation and Isotopes*, 28(10), 855–860, [https://doi.org/10.1016/0020-708X\(77\)90026-6](https://doi.org/10.1016/0020-708X(77)90026-6), 1977.
- Opazo, T., Aravena, R., and Parker, B.: Nitrate distribution and potential attenuation mechanisms of a municipal water supply bedrock aquifer, *Applied Geochemistry*, 73, 157–168, <https://doi.org/10.1016/j.apgeochem.2016.08.010>, 2016.
- Pangle, L. A., Kim, M., Cardoso, C., Lora, M., Meira Neto, A. A., Volkmann, T. H. M., Wang, Y., Troch, P. A., and J., H. C.: The mechanistic basis for storage-dependent age distributions of water discharged from an experimental hillslope, *Water Resour. Res.*, 53, 2733–2754, 580 <https://doi.org/10.1002/2016WR019901>, 2017.
- Queloz, P., Carraro, L., Benettin, P., Botter, G., Rinaldo, A., and Bertuzzo, E.: Transport of fluorobenzoate tracers in a vegetated hydrologic control volume: 2. Theoretical inferences and modeling., *Water Resour. Res.*, 51, 2793–2806, <https://doi.org/10.1002/2014WR016508>, 2015.
- Rinaldo, A. and Marani, M.: Basin Scale Model of Solute Transport, *Water Resour. Res.*, 23, 2107–2118, 585 <https://doi.org/10.1029/WR023i011p02107>, 1987.
- Rinaldo, A., Botter, G., Bertuzzo, E., Uccelli, A., Settin, T., and Marani, M.: Transport at basin scales: 1. Theoretical framework, *Hydrol. Earth Syst. Sci.*, 10, 19–29, <https://doi.org/10.5194/hess-10-19-2006>, 2006.
- Rinaldo, A., Benettin, P., Harman, C. J., Hrachowitz, M., McGuire, K. J., van der Velde, Y., et al.: Storage selection functions: A coherent framework for quantifying how catchments store and release water and solutes, *Water Resour. Res.*, 51, 4840–4847, 590 <https://doi.org/10.1002/2015WR017273>, 2015.
- Rodriguez, N. B., McGuire, K. J., and Klaus, J.: Time-Varying Storage–Water Age Relationships in a Catchment With a Mediterranean Climate, *Water Resour. Res.*, 54, 3988–4008, <https://doi.org/10.1029/2017WR021964>, 2018.
- Rodriguez, N. B., Pfister, L., Zehe, E., and Klaus, J.: A comparison of catchment travel times and storage deduced from deuterium and tritium tracers using StorAge Selection functions, *Hydrol. Earth Syst. Sci.*, 25, 401–428, <https://doi.org/10.5194/hess-25-401-2021>, 2021.
- 595 Rodríguez-Cruz, M. S., Jones, J. E., and Bending, G. D.: Field-scale study of the variability in pesticide biodegradation with soil depth and its relationship with soil characteristics, *Soil Biology and Biochemistry*, 38, 2910–2918, <https://doi.org/10.1016/j.soilbio.2006.04.051>, 2006.
- Samaniego, L., Kumar, R., and Attinger, S.: Multiscale parameter regionalization of a grid-based hydrologic model at the mesoscale, *Water Resour. Res.*, 46, W05 523, <https://doi.org/10.1029/2008WR007327>, 2010.
- Schoups, G., van de Giesen, N. C., and Savenije, H. H. G.: Model complexity control for hydrologic prediction, *Water Resour. Res.*, 44, 600 W00B03, <https://doi.org/10.1029/2008WR006836>, 2008.
- Seeger, S. and Weiler, M.: Reevaluation of transit time distributions, mean transit times and their relation to catchment topography, *Hydrol. Earth Syst. Sci.*, 18, 4751–4771, <https://doi.org/10.5194/hess-18-4751-2014>, 2014.





- Soulsby, C., Tetzlaff, D., Rodgers, P., Dunn, S., and Waldron, S.: Runoff processes, stream water residence times and controlling landscape characteristics in a mesoscale catchment: An initial evaluation, *J. Hydrol.*, 325, 197–221, <https://doi.org/10.1016/j.jhydrol.2005.10.024>, 605 2006.
- Sprenger, M., Seeger, S., Blume, T., and Weiler, M.: Travel times in the vadose zone: Variability in space and time, *Water Resour. Res.*, 52, 5727–5754, <https://doi.org/10.1002/2015WR018077>, 2016.
- Stewart, M. K., Morgenstern, U., and McDonnell, J. J.: Truncation of stream residence time: How the use of stable isotopes has skewed our concept of streamwater age and origin, *Hydrol. Process.*, 24, 1646–1659, <https://doi.org/10.1002/hyp.7576>, 2010.
- 610 Stewart, M. K., Morgenstern, U., McDonnell, J. J., and Pfister, L.: The ‘hidden streamflow’ challenge in catchment hydrology: A call to action for stream water transit time analysis, *Hydrol. Process.*, 26, 2061–2066, <https://doi.org/10.1002/hyp.9262>, 2012.
- Stockinger, M. P., Lücke, A., McDonnell, J. J., Diekkrüger, B., Vereecken, H., and Bogena, H. R.: Interception effects on stable isotope driven streamwater transit time estimates, *Geophys. Res. Lett.*, 42, 5299–5308, <https://doi.org/doi:10.1002/2015GL064622>, 2015.
- Stockinger, M. P., Bogena, H. R., Lücke, A., Diekkrüger, B., Cornelissen, T., and Vereecken, H.: Tracer sampling fre-  
615 quency influences estimates of young water fraction and streamwater transit time distribution, *J. Hydrol.*, 541, 952–964, <https://doi.org/10.1016/j.jhydrol.2016.08.007>, 2016.
- Sutanudjaja, E. H., Van Beek, R., Wanders, N., Wada, Y., Bosmans, J. H. C., et al.: PCR-GLOBWB 2: a 5 arcmin global hydrological and water resources model, *Geosci. Model Dev.*, 11, 2429–2453, <https://doi.org/10.5194/gmd-11-2429-2018>, 2018.
- Svensson, T., Lovett, G. M., and Likens, G. E.: Is chloride a conservative ion in forest ecosystems?, *Biogeochemistry*, 107, 125–134,  
620 <https://doi.org/10.1007/s10533-010-9538-y>, 2012.
- Tetzlaff, D., Piovano, T., A., P., Smith, A., K., C. S., Marsh, P., Wookey, P. A., Street, L. E., and Soulsby, C.: Using stable isotopes to estimate travel times in a data-sparse Arctic catchment: Challenges and possible solutions, *Hydrol. Process.*, 32, 1936–1952, <https://doi.org/10.1002/hyp.13146>, 2018.
- Thiemig, V., Rojas, R., Zombrano-Bigiarini, M., and De Roo, A.: Hydrological evaluation of satellite-based rainfall estimates over the Volta  
625 and Baro-Akobo Basin, *J. Hydrol.*, 499, 324–338, <https://doi.org/10.1016/j.jhydrol.2013.07.012>, 2013.
- Timbe, E., Windhorst, W., Celleri, R., Timbe, L., Crespo, R., Frede, H. G., Feyen, J., and Breuer, L.: Sampling frequency trade-offs in the assessment of mean transit times of tropical montane catchment waters under semi-steady-state conditions, *Hydrol. Earth Syst. Sci.*, 19, 1153–1168, <https://doi.org/10.5194/hess-19-1153-2015>, 2015.
- Van der Velde, Y., De Rooij, G. H., Rozemeijer, J. C., Van Geer, F. C., and Broers, H. P.: Nitrate response of a lowland catch-  
630 ment: On the relation between stream concentration and travel time distribution dynamics, *Water Resour. Res.*, 46, W11534, <https://doi.org/10.1029/2010WR009105>, 2010.
- van der Velde, Y., Torfs, P. J. J. F., van der Zee, S. E. A. T. M., and Uijlenhoet, R.: Quantifying catchment-scale mixing and its effect on time-varying travel time distributions, *Water Resour. Res.*, 48, W06536, <https://doi.org/10.1029/2011WR011310>, 2012.
- Van Meter, K. J., Basu, N. B., and Van Cappellen, P.: Two centuries of nitrogen dynamics: legacy sources and sinks in the Mississippi and  
635 Susquehanna river basins, *Global Biogeochemical Cycles*, 31, 2–23, <https://doi.org/10.1002/2016GB005498>, 2017.
- Visser, A., Broers, H. P., Purtschert, R., Sültenfuß, J., and de Jonge, M.: Groundwater age distributions at a public drinking water supply well field derived from multiple age tracers (85Kr, 3H/3He, and 39Ar), *Water Resour. Res.*, 49, 7778–7796, <https://doi.org/10.1002/2013WR014012>, 2013.



- 640 Visser, A., Thaw, M., Deinhart, A., Bibby, R., Safeeq, M., Conklin, M., Esser, B., and van der Velde, Y.: Cosmogenic isotopes unravel the hydrochronology and water storage dynamics of the Southern Sierra critical zone, *Water Resour. Res.*, 55, 1429–1450, <https://doi.org/10.1029/2018WR023665>, 2019.
- von Freyberg, J., Studer, B., and Kirchner, J. W.: A lab in the field: high-frequency analysis of water quality and stable isotopes in stream water and precipitation, *Hydrol. Earth Syst. Sci.*, 21, 1721–1739, <https://doi.org/10.5194/hess-21-1721-2017>, 2017.
- 645 von Freyberg, J., Allen, S. T., Seeger, S., Weiler, M., and Kirchner, J. W.: Sensitivity of young water fractions to hydro-climatic forcing and landscape properties across 22 Swiss catchments, *Hydrol. Earth Syst. Sci.*, 22, 3841–3861, <https://doi.org/10.5194/hess-22-3841-2018>, 2018.
- von Freyberg, J., Rücker, A., Zappa, M., Schlumpf, A., Studer, B., and Kirchner, J. W.: Four years of daily stable water isotope data in stream water and precipitation from three Swiss catchments, *Sci Data*, 9, 46, <https://doi.org/10.1038/s41597-022-01148-1>, 2022.
- Wilusz, D. C., Harman, C. J., and Ball, W. P.: Sensitivity of Catchment Transit Times to Rainfall Variability Under Present and Future  
650 Climates, *Water Resour. Res.*, 53, 10 231–10 256, <https://doi.org/10.1002/2017WR020894>, 2017.
- Wilusz, D. C., Harman, C. J., Ball, W. P., Maxwell, R. M., and Buda, A. R.: Using Particle Tracking to Understand Flow Paths, Age Distributions, and the Paradoxical Origins of the Inverse Storage Effect in an Experimental Catchment, *Water Resour. Res.*, 56, e2019WR025 140, <https://doi.org/10.1029/2019WR025140>, 2020.
- 655 Winter, C., Lutz, S. R., Musolff, A., Kumar, R. Weber, M., and Fleckenstein, J. H.: Disentangling the Impact of Catchment Heterogeneity on Nitrate Export Dynamics From Event to Long-Term Time Scales, *Water Resour. Res.*, 57, e2020WR027 992, <https://doi.org/10.1029/2020WR027992>, 2020.
- Wollschläger, U., Attinger, S., Borchardt, D., Brauns, M., Cuntz, M., Dietrich, P., et al.: The Bode hydrological observatory: a platform for integrated, interdisciplinary hydro-ecological research within the TERENO Harz/Central German Lowland Observatory, *Environmental Earth Sciences*, 76, 29, <https://doi.org/10.1007/s12665-016-6327-5>, 2017.
- 660 Xu, G., Magen, H., Tarchitzky, J., and Kafkafi, U.: Advances in Chloride Nutrition of Plants, *Adv. Agron.*, 68, 97–150, [https://doi.org/10.1016/S0065-2113\(08\)60844-5](https://doi.org/10.1016/S0065-2113(08)60844-5), 1999.
- Zink, M., Kumar, R., Cuntz, M., and Samaniego, L.: A high-resolution dataset of water fluxes and states for Germany accounting for parametric uncertainty, *Hydrol. Earth Syst. Sci.*, 21, 1769–1790, <https://doi.org/10.5194/hess-21-1769-2017>, 2017.